cbecimat26
26° Congresso Brasileiro de Engenharia e Ciência dos Materiais
22 a 26 de novembro de 2026
Costão do Santinho
Florianópolis-SC

Longitudinal wave attenuation in mechanical metamaterial rods with periodic shunted piezo-patches

BRITO, M. L.[1]; SALES, M. B. M.[2]; PROTÁZIO, S.P.[1]; COELHO J. J. S.[1]; DOS SANTOS, J. M. C.[2]; MIRANDA JR., E. J. P.[1,2]

Graduate Program in Materials Science and Technology, Federal Institute of Education, Science, and Technology of Maranhão, São Luís, MA, and [2]Graduate Program in Mechanical Engineering, University of Campinas, Campinas, SP

edson.jansen@ifma.edu.br

INTRODUCTION

- Piezoelectric effect;
- Attenuation at low frequencies using different piezoelectric materials;
- Band gaps with Bragg scattering.

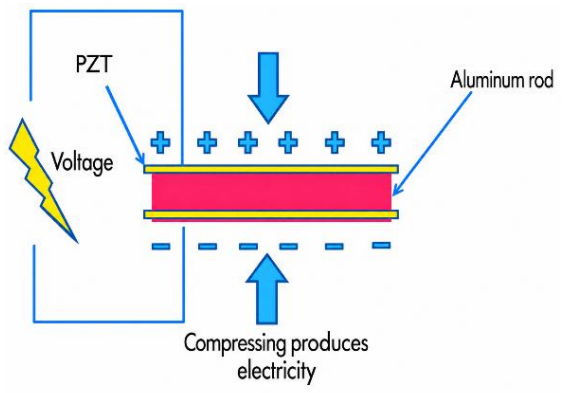


Figure 1: Piezoelectricity.

ROD MODELLING

- Software COMSOL Multiphysics based on FEM.

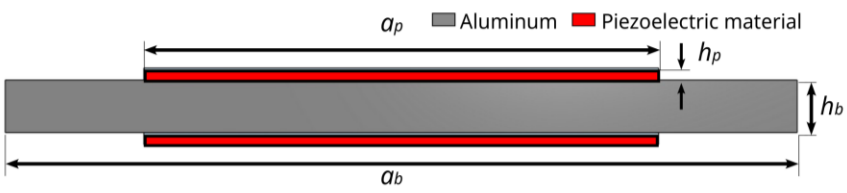


Figure 2: Schematic representation of the aluminum rod (gray) with bonded piezoelectric material (red): (a) unit-cell model, showing the rod length a_b and height h_b, and the PZT length a_p and height h_p.

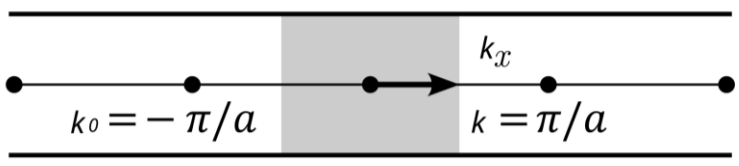


Figure 3: Representation of the first Brillouin zone (FBZ) and the wavenumber k_x.

- Semi-analytical PWE and EPWE methods for the complex dispersion diagrams.
- Numerical forced response and real dispersion diagram based on FEM.
- Electrical conditions: open circuit (OC) and short circuit (SC).

Table 1: Geometry and properties of the system composed of the aluminum (6061) rod (b) and the PZT (p) (Miranda Jr. et al., 2021).

Geometry/Property	Value
Length of the aluminum rod (a_b)	0.054 m
Length of the piezoelectric arrangement (a_p)	0.0351 m
Thickness of the aluminum rod (h_b)	0.0035 m
Thickness of the piezoelectric arrangement (h_b)	0.0008 m
Mass density of aluminum rod (ρ_b)	2700 kg/m^3
Mass density of the piezoelectric material (ρ_p)	7800 kg/m^3
Young's modulus of aluminum (E_b)	69 GPa
Young's modulus of the piezoelectric material (E_p)	63 GPa

NUMERICAL RESULTS

Table 2: Physical parameters of piezoelectric materials (B).

Geometry/Property	Value
Filling fraction (f)	0.65
Mass density ($\rho_{B2}, \rho_{B3}, \rho_{B4}, \rho_{B5}$)	5900 kg/m^3, 4500 kg/m^3, 8100 kg/m^3, 8200 kg/m^3
Young's modulus ($E_{B2}, E_{B3}, E_{B4}, E_{B5}$)	130 GPa, 120 GPa, 55 GPa, 50 GPa
Electromechanical coupling coefficient (k_{31})	0.35

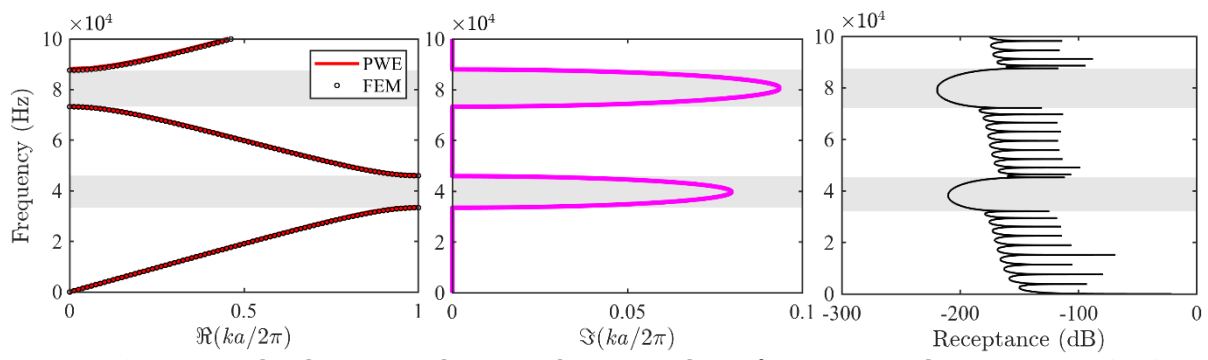


Figure 4: Real and imaginary dispersion diagrams and FRF for **PZT-5A** under **open-circuit (OC)** conditions, where for the FEM and PWE, the first bandgap extends from 33296 to 45953 Hz, whereas the second occurs between 73217 and 87633 Hz. EPWE, with approximate values of 0.079 and 0.093, respectively. FRF, within the first bandgap with minimum receptance of approximately -210.170 dB was observed at 38203 Hz and of -219.710 dB at 79957 Hz for the second bandgap.

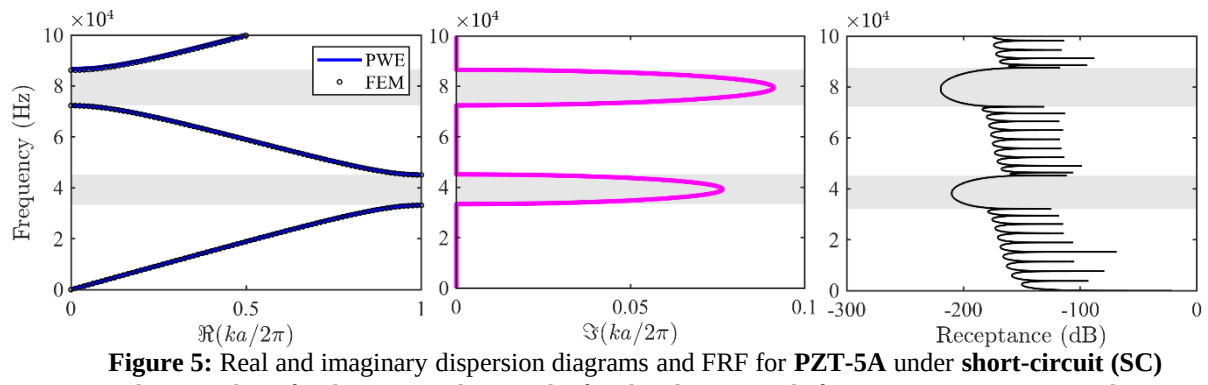


Figure 5: Real and imaginary dispersion diagrams and FRF for **PZT-5A** under **short-circuit (SC)** conditions, where for the FEM and PWE, the first bandgap extends from 33107 to 45058 Hz, whereas the second occurs between 72296 and 86220 Hz. EPWE, with approximate values of 0.076 and 0.091, respectively. FRF, within the first bandgap with minimum receptance of approximately -210.170 dB was observed at 38188 Hz and for the second bandgap -219.710 dB at 79243 Hz.

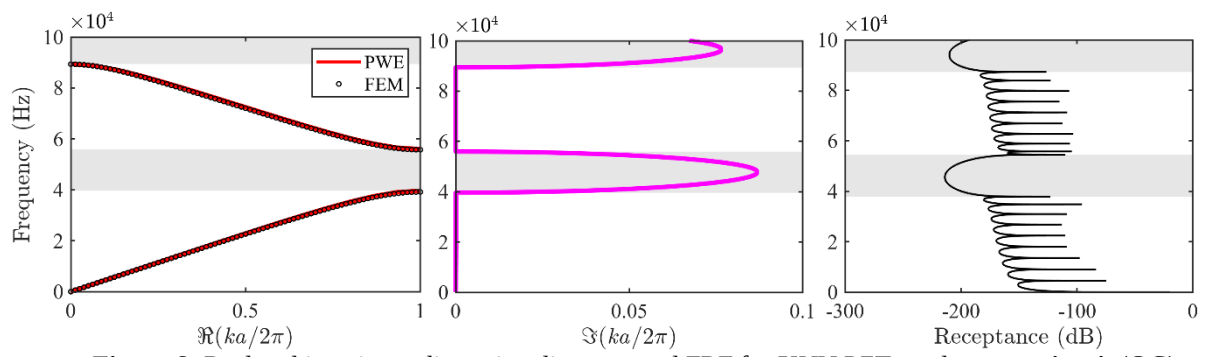


Figure 6: Real and imaginary dispersion diagrams and FRF for **KNN** PZTs under **open-circuit (OC)** conditions. The FEM and PWE results exhibit two bandgaps under both electrical conditions. The EPWE exhibits maxima of the imaginary part of the wave number of approximately 0.086 and 0.076. The FRFs, the first bandgap exhibits a minimum receptance of approximately -214.010 dB at 45586 Hz, and the second bandgap of approximately -210.280 dB at 94054 Hz.

Table 3: Comparison of piezoelectric materials under different electrical conditions.

PZT Material	Electrical condition	1st Bandwidth (Hz)	1st Midgap (Hz)	Max. Im (k)	Min. Receptance (dB)	2nd Bandwidth (Hz)	2nd Midgap (Hz)	Max. Im (k)	Min. Receptance (dB)
5A	OC	12657	38203	0.079	-210.170	14416	79957	0.093	-219.710
	SC	11951	38188	0.076	-210.170	13923	79243	0.091	-219.710
BNT	OC	17904	44041	0.097	-219.560	15069	91192	0.091	-214.010
	SC	16606	44170	0.091	-219.560	14726	94054	0.089	-214.010
KNN	OC	16571	45586	0.086	-214.010	12905	94054	0.076	-210.243
	SC	15311	45580	0.081	-214.010	12614	94009	0.074	-210.243
PMN-PT	OC	11926	37816	0.077	-208.340	14071	78250	0.093	-218.580
	SC	11373	37636	0.074	-208.340	13652	78049	0.090	-218.580
PZN-PT	OC	11548	37423	0.075	-207.067	13725	77458	0.092	-217.732
	SC	10993	37378	0.072	-207.067	13401	77482	0.089	-217.732

CONCLUSIONS

- Open-circuit condition consistently produces slightly wider bandgaps shifted toward higher frequencies;
- PMN-PT and PZN-PT favored bandgap formation at relatively lower frequencies;
- BNT exhibited the highest spatial decay rate for evanescent waves, while PZN-PT, under short-circuit conditions, produced a minimum receptance comparable to that obtained for PZT-5A.

ACKNOWLEDGEMENTS

Funds from FAPEMA (Grant Reference Number BM-03266/25).